EPJ manuscript No.
(will be inserted by the editor)

Study of ambiguities in $\pi^- p \to \Lambda K^0$ scattering amplitudes

A.V. Anisovich [1,2], R. Beck [1], E. Klempt [1], V.A. Nikonov [1,2], A.V. Sarantsev [1,2], U. Thoma [1], and Y. Wunderlich [1]

[1] Helmholtz-Institut für Strahlen- und Kernphysik, Universität Bonn, Germany
[2] Petersburg Nuclear Physics Institute, Gatchina, Russia

December 3, 2024

arXiv:1306.5126v1 [hep-ph] 21 Jun 2013

Abstract. Amplitudes for the reaction $\pi^- p \to \Lambda K^0$ are reconstructed from data on the differential cross section $d\sigma/d\Omega$, the recoil polarization P, and on the spin rotation parameter β. At low energies, no data on β exist, resulting in ambiguities. An approximation using S and P waves leads only to a fair description of the data on $d\sigma/d\Omega$ and P; in this case, there are two sets of amplitudes. Including D waves, the data on $d\sigma/d\Omega$ and P are well reproduced by the fit but now, there are several distinct solutions which describe the data with identical precision. In the range where the spin rotation parameter β was measured, a full and unambiguous reconstruction of the partial wave amplitudes is possible. The energy-independent amplitudes are compared to the energy dependent amplitudes which resulted from a coupled channel fit (BnGa2011-02) to a large data set including both pion and photo-induced reactions. Significant deviations are observed. Consistency between energy dependent and energy independent solutions by choosing the energy independent solution which is closest to the energy dependent solution. In a second step, the *known* energy dependent solution for low (or high) partial waves is imposed and only the high (or low) partial waves are fitted leading to smaller uncertainties.

PACS: 11.80.Et, 11.80.Gw, 13.30.-a, 13.30.Ce, 13.30.Eg, 13.60.Le 14.20.Gk

1 Introduction

The excitation spectrum of the nucleon has been studied in experiments on πN elastic scattering, including experiments in which the target nucleon is polarized or in which the recoil polarization of the scattered nucleon is measured in a secondary reaction. Data on the $\pi^- p \to n\pi^+$ charge exchange are required to separate the two isospin contributions. Elastic scattering yields differential cross sections $d\sigma/d\Omega$. A transversely polarized target - or the decay asymmetry of hyperons in the final state - can be used to determine the analyzing power P, the spin transfer from a nucleon polarized longitudinally (along the pion beam line) to the final state baryon yields the spin rotation parameters A and R or the spin rotation angle $\beta = \arctan(-R/A)$. $d\sigma/d\Omega$ and two polarization observables need to be known to reconstruct the scattering amplitude without using further constraints; the third polarization variable can be calculated up to a sign ambiguity from the relation

$$P^2 + A^2 + R^2 = 1. \quad (1)$$

In practice, experimental information on the spin rotation parameters A and R is mostly missing. In this case, the scattering amplitude is not defined unambiguously [1]. A unique solution can be constructed using constraints from dispersion relations linking the real and the imaginary part of the scattering amplitude [2,3,4]. One can get a limited number of different solutions without the use of theoretical input, by fitting the data with Legendre polynomials (with a finite number of coefficients) which provide a link between data at different angles.

Alternatively, the ambiguity problem can be solved by starting from an energy-dependent fit to the data [5]. In an energy-dependent fit, the amplitudes are constrained by analytic functions in energy and angle. The ambiguity problem can be solved by selecting a solution which is compatible with the amplitude determined from the energy-dependent fit. The amplitudes from the energy-independent solution can then be used as input for an iterative procedure [5]. The energy independent solution thus obtained is then the correct one, provided that the energy dependent amplitudes were close to the correct values. In a recent article, these methods were applied to the reactions $\pi^- p \to p\eta$ and $\pi^- p \to \Lambda K^0$. Energy independent solutions for the S_{11}, P_{11}, P_{13}, D_{15}, F_{15}, and F_{17} amplitudes were given [6] and used to extract parameters of contributing resonances in a multichannel analysis [7].

In this article we restrict ourselves to the reaction $\pi^- p \to \Lambda K^0$ using the data from [8,9,10,11]. Our aim here is however not to determine the $\pi^- p \to \Lambda K^0$ scattering amplitudes but rather to study the ambiguities which are intrinsic parts of the method when the data are incomplete and of limited accuracy.

2 Pion induced reaction

2.1 Amplitudes, partial waves and observables

Scattering processes of a pseudoscalar meson off a nucleon to a final state with a pseudoscalar meson plus a spin-1/2 baryon are conventionally described in terms of a scattering matrix M

with the following structure in the reaction center-of-mass system

$$M = f(W,z) + g(W,z) i(\vec{\sigma}\vec{n}) \tag{2}$$

where $f(W,z)$ is the non-spin-flip amplitude, $g(W,z)$ is the spin-flip amplitude, $\vec{n}$ is the normal vector of the production plane and $\vec{\sigma}$ are the Pauli spin matrices. The amplitudes $f(W,z)$ and $g(W,z)$ depend on total energy W and on $z = \cos\Theta$ where Θ is the scattering angle of the outgoing meson in the center-of-mass system (cms). The normal vector of the production plane is defined as

$$\vec{n} = \frac{\vec{q} \times \vec{k}}{|\vec{q} \times \vec{k}|}, \tag{3}$$

where $\vec{q}$ is the initial cms momentum of the meson, q its modulus, $\vec{k}$ is the final meson cms momentum, k its modulus. The amplitudes f and g can be expanded into partial waves

$$f(W,z) = \frac{1}{\sqrt{qk}} \sum_{l=0}^{L} \left[(l+1)A_l^+(W) + lA_l^-(W)\right] P_l(z) \ ,$$
$$g(W,z) = \frac{1}{\sqrt{qk}} \sin\Theta \sum_{l=1}^{L} \left[A_l^+(W) - A_l^-(W)\right] P_l'(z) \ . \tag{4}$$

The partial amplitudes $A_l^\pm$ depend only on the total energy W of the reaction, the A_l^+ functions describe the $1/2^-$, $3/2^+$, $5/2^-$, ... states and the A_l^- functions the $1/2^+$, $3/2^-$, $5/2^+$, ... states. P_l are Legendre polynomials in z and P_l' are their derivatives. The initial πN system has isospin $I = 1/2$ and $I = 3/2$ and the amplitudes $A_l^\pm$ can be decomposed into the isospin amplitudes as follows:

$$A_l^\pm = C_{\frac{1}{2}} A_{l\frac{1}{2}}^\pm + C_{\frac{3}{2}} A_{l\frac{3}{2}}^\pm \ . \tag{5}$$

For reaction $\pi^- p \to \Lambda K^0$ $C_{\frac{1}{2}} = -\sqrt{\frac{2}{3}}$ and $C_{\frac{3}{2}} = 0$.

The amplitudes f and g are complex functions. Except for an arbitrary phase, f and g can be calculated up to one discrete ambiguity when three observables are known. These can be chosen to be the differential cross section $d\sigma/d\Omega$, the polarization P of the outgoing baryon in the final state, and spin-rotation angle β. The differential cross section is given by

$$\frac{d\sigma}{d\Omega} = \frac{k}{q}(|f|^2 + |g|^2) \ , \tag{6}$$

and the total cross section is

$$\sigma = \frac{2\pi}{q^2}(2J+1) \sum_{l=0}^{L} \left[|A_l^+(W)|^2 + |A_l^-(W)|^2\right] \tag{7}$$

where J is the total spin of the state (remember that $J = |l \pm 1/2|$ for $\pm$ states).

The polarization in the final state is given by

$$P = \frac{-2Im(f^* g)}{|f|^2 + |g|^2} \ . \tag{8}$$

The third observable is the spin-rotation angle:

$$\beta = arg\Big(\frac{f - ig}{f + ig}\Big) = tan^{-1}\Big(\frac{-2Re(f^* g)}{|f|^2 - |g|^2}\Big) \ . \tag{9}$$

In some pion-induced experiments not the β angle was measured but one or both spin-rotation parameters, R and A. They are defined as

$$R = \frac{2Re(f^* g)}{|f|^2 + |g|^2} \ , \quad A = \frac{|f|^2 - |g|^2}{|f|^2 + |g|^2} \ . \tag{10}$$

P, R and A are not the independent observables. The polarization variables are constrained by the relation 1.

2.2 Amplitude ambiguities when only $d\sigma/d\Omega$ and P are known

Often, only the observables $d\sigma/d\Omega$ and P are measured. We face this situation even in the simplest case of πN elastic scattering. The target nucleon can be polarized transversely giving access to P. Experimentally more difficult are measurements of the spin rotation parameters A and R. Their determination requires to measure the proton polarization in a secondary scattering process. Therefore, A and R have been determined only in a rather limited range of energies and angle. In the case of pion-induced hyperon production ($K\Lambda$ or $K\Sigma$), the analyzing power P of the final-state hyperon can be inferred from its decay, and only no secondary scattering process is required for a complete experiment. The spin rotation variables can then be determined using a target which is polarized longitudinally. Also here, the data covers only a limited range in energy and solid angle.

The problem of ambiguities in the case of so-called "incomplete" experiments (with lack of spin-rotation information) has been discussed many decades ago, see [12,13,14]. Let us briefly remind of the origin of such ambiguities. The cross section with polarization information (assuming that the target nucleon is fully polarized) can be defined as

$$(1 \pm P)\frac{d\sigma}{d\Omega} = |f \pm ig|^2. \tag{11}$$

The idea is to replace the two functions $(1 \pm P)\frac{d\sigma}{d\Omega}$ by a single function. To do this we expand the physical region of the scattering angle Θ from $[0,\pi]$ to $[0,2\pi]$. Using a new variable $w = e^{i\Theta}$ one can see that the f amplitude is even in power of w and w^{-1} since it depends on $z = \frac{1}{2}(w + w^{-1})$. The g amplitude contains $\sin\Theta = \frac{1}{2i}(w - w^{-1})$ and so behaves as $g(w^{-1}) = -g(w)$. Let us define the function

$$F(w) = f(w) + ig(w) \ . \tag{12}$$

For $\Theta \epsilon [0,\pi]$

$$F(w) = f(z) + ig(z) \ , \quad |F(w)|^2 = (1+P)\frac{d\sigma}{d\Omega} \tag{13}$$

holds. For $\Theta \epsilon [\pi, 2\pi]$, $\sin\Theta < 0$ and $g(w) = -g(z)$, hence

$$F(w) = f(z) - ig(z) \ , \quad |F(w)|^2 = (1-P)\frac{d\sigma}{d\Omega} \ . \tag{14}$$

Instead of a real and positive cross section in the region $-1 \leq z \leq 1$ (the case of scalar particle rescattering), we now have a real and positive cross section in the region $0 \leq \Theta \leq 2\pi$ or on the unit circle of the w plane.

Let us rewrite $|F(w)|^2$ as a power series in w:

$$|F(w)|^2 = \sum_{n=-N}^{N} a_n w^n \tag{15}$$

where N depends on maximal orbital momentum L in eq. (4). Since $|F(w)|^2$ is real on the unit circle in the w-plane, we can write this function as a product of roots in the following form

$$|F(w)|^2 = C \prod_{i=1}^{N} (w - w_i)(w^{-1} - w_i^*) \,. \tag{16}$$

Remember that $w^* = w^{-1}$ on the unit circle. Finally we have

$$F(w) = C^{\frac{1}{2}} e^{i\phi} \prod_{i=1}^{N} (w - w_i) \,. \tag{17}$$

Equation (17) is not the only possible solution, one can as well take $(w - w_i)$ or $(w^{-1} - w_i^*)$ as a root, and this gives 2^N different solutions. But not all of these solution are physically sensible. In the next section we discuss the ambiguities in the case when only a limited number of amplitudes are taken into account.

2.3 Amplitude near the threshold

We could expect that near threshold only S and P waves are important. As a simple and educative example let us consider the case of two waves with $J^P = 1/2^-$ and $1/2^+$ only. Let us denote the magnitude and phase of the scattering amplitude as $r_{l\pm}$ and $\phi_{l\pm}$, respectively. Since each amplitude can be multiplied by a factor $e^{i\Phi}$ without changing the observables, we set $\phi_{0+} = 0$ for simplicity. The cross section and polarization in the final state can be calculated as

$$\frac{d\sigma}{d\Omega} = \frac{k}{q}\, I_0 \qquad \text{and} \tag{18}$$

$$P\, I_0 = 2 \sin\Theta\; r_{0+} r_{1-} \sin(\phi_{1-}) \tag{19}$$

where

$$I_0 = r_{0+}^2 + r_{1-}^2 + 2z \cos(\phi_{1-}) r_{0+} r_{1-} \,. \tag{20}$$

The interference of the $1/2^-$ and $1/2^+$ waves leads to a linear dependence of the differential cross section in z while the recoil asymmetry multiplied with the differential cross section and divided by $\sin\Theta$ should be flat. Using eqs.(13 - 15), we can write the amplitude magnitude square $|F(w)|^2$ as

$$|F(w)|^2 = \sum_{i=-1}^{1} a_i^{\pm}\, w^i \tag{21}$$

where

$$a_{-1}^{\pm} = r_{0+} r_{1-} (\cos(\phi_{1-}) \pm i \sin(\phi_{1-})) \,, \tag{22}$$

$$a_0^{\pm} = r_{0+}^2 + r_{1-}^2 \,, \quad a_1^{\pm} = (a_{-1}^{\pm})^* \,. \tag{23}$$

The coefficients a_i^+ define the amplitude $F(w)$ in the region $0 \leq \Theta \leq \pi$, while the a_i^- define $F(w)$ in the region $\pi \leq \Theta \leq 2\pi$. The expressions above clearly demonstrate the ambiguity in the determination of $1/2^-$ and $1/2^+$ waves: they cannot be distinguished. Any PWA solution with dominant $1/2^-$ and $1/2^+$ waves has an alternative solution where the magnitudes of S and P waves replace each other.

The more general case includes another P wave, $J^P = 3/2^+$. The cross section and polarization in the final state can be calculated as

$$\frac{d\sigma}{d\Omega} = \frac{k}{q}\, I_0 \tag{24}$$

$$\begin{aligned} P\, I_0 = 2 \sin\Theta\, (r_{1-} r_{0+} \sin(\phi_{1-}) + \\ r_{1+}(3z r_{1-} \sin(\phi_{1-} - \phi_{1+}) - r_{0+} \sin(\phi_{1+}))) \end{aligned} \tag{25}$$

where

$$\begin{aligned} I_0 = r_{1-}^2 + 2z \cos(\phi_{1-}) r_{1-} r_{0+} + r_{0+}^2 + \\ 2(-1 + 3z^2) \cos(\phi_{1-} - \phi_{1+}) r_{1-} r_{1+} + \\ 4z \cos(\phi_{1+}) r_{0+} r_{1+} + r_{1+}^2 + 3z^2 r_{1+}^2 \,. \end{aligned} \tag{26}$$

Here, the differential cross section has a z^2 term while the polarization multiplied by the differential cross section and divided by $\sin\Theta$ has a z term. The amplitude magnitude square $|F(w)|^2$ can be calculated as

$$|F(w)|^2 = \sum_{i=-2}^{2} a_i^{\pm}\, w^i \tag{27}$$

where

$$\begin{aligned} a_{-2}^{\pm} = 3/4 r_{1+} (2 \cos(\phi_{1-} - \phi_{1+}) r_{1-} + \\ r_{1+} \pm 2i\, r_{1-} \sin(\phi_{1-} - \phi_{1+})) \end{aligned} \tag{28}$$

$$\begin{aligned} a_{-1}^{\pm} = r_{0+} (\cos(\phi_{1-}) r_{1-} + 2 \cos(\phi_{1+}) r_{1+} \pm \\ i(r_{1-} \sin(\phi_{1-}) - r_{1+} \sin(\phi_{1+}))) \end{aligned} \tag{29}$$

$$a_0^{\pm} = r_{1-}^2 + r_{0+}^2 + \cos(\phi_{1-} - \phi_{1+}) r_{1-} r_{1+} + \frac{5}{2} r_{1+}^2 \tag{30}$$

$$a_1^{\pm} = (a_{-1}^{\pm})^* \,, \quad a_2^{\pm} = (a_{-2}^{\pm})^* \tag{31}$$

Equations (28 - 30) can be used to search for ambiguities. For any found solution we can write a system of equations $a_i^{\pm}(r_{l\pm}, \phi_{l\pm}) = C_i$. In this particular case we have five equations for the real and imaginary part of $a_i^{\pm}$ which define additional allowed solutions for the $r_{l\pm}$ and $\phi_{l\pm}$.

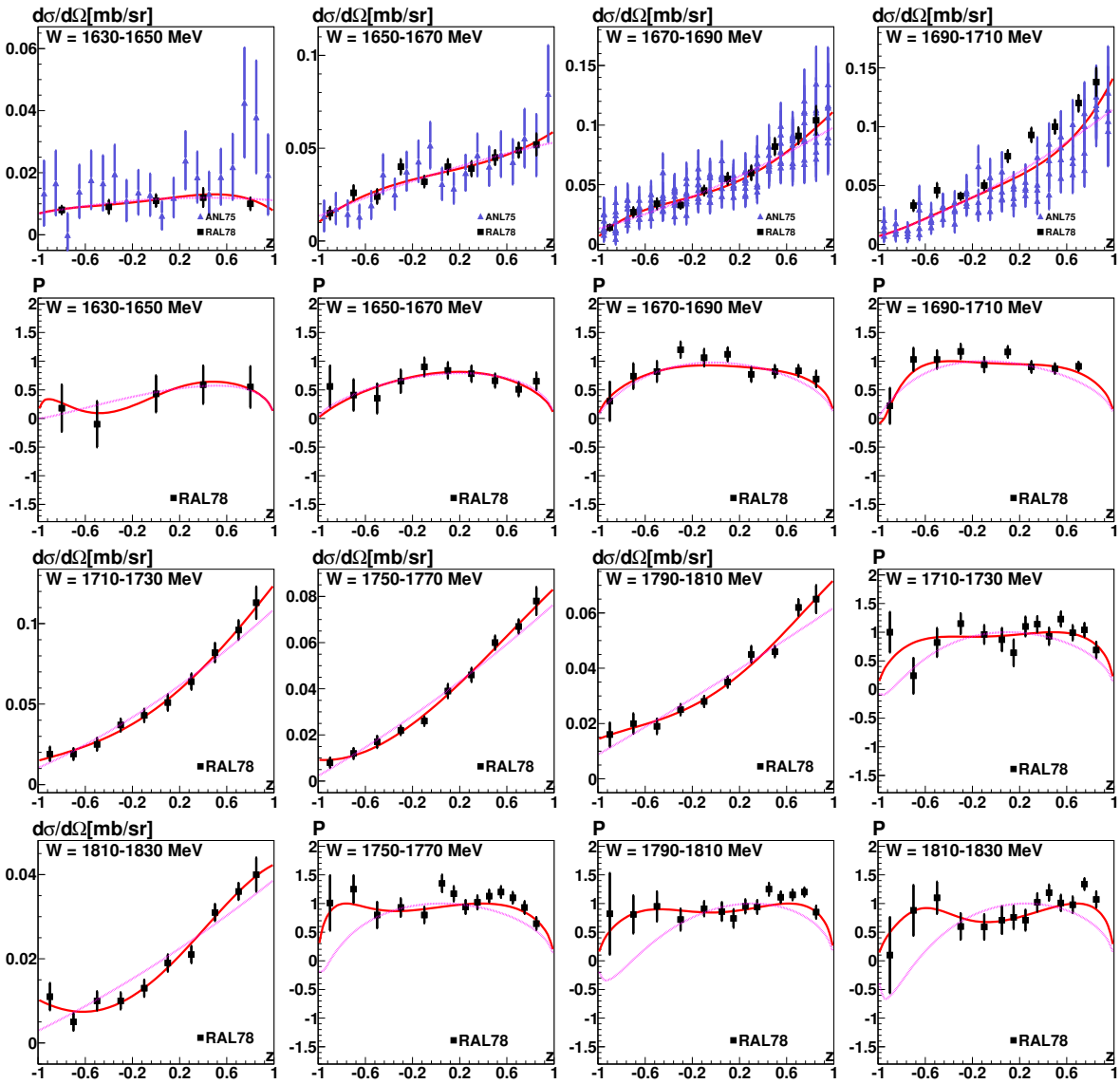

Fig. 1. Differential cross sections and Λ polarization for the reaction $\pi^- p \to K^0 \Lambda$ from ANL75 (blue) [8] and RAL78 (black) [9]. Note that a few differential cross sections from [8] fall into a single energy window. The data are compared to two fits using S and P waves (red dotted line) and with S, P and D waves (red solid line). The BnGa2010-02 fit to the data is shown in figs. 1 - 4 of [15].

3 Energy-independent PWA near threshold

We first consider an energy independent fit to data from the reaction $\pi^- p \to \Lambda K^0$ in the energy region below $W = 1830$ MeV. Experimental data on this reaction are available for $d\sigma/d\Omega$, $Pd\sigma/d\Omega$ and P [8,9]. The experimental data, divided into 20 MeV bins, are shown on Fig. 1. In this region the differential cross section has some small z^2 dependence, hence we expect that at least three partial waves need to be included: S_{11}, P_{11} and P_{13}. We then compare our energy independent solutions with an energy dependent solution. The latter was obtained from a multichannel fit to a large body of photo- and pion-induced reactions [16].

3.1 Energy independent PWA near threshold with S and P waves

The data were fitted with this hypothesis, the fit is shown by a dotted line in Fig. 1; the quality of the fit for each energy bin is given in Table 1.

In the lowest energy region, below 1700 MeV, the fit agrees reasonably well with the data but significant deviations between data and fit are observed above this energy. Hence we expect that higher partial waves are needed, at least above 1700 MeV. Nevertheless, we determined the amplitudes from this fit.

The amplitudes for the S_{11}, P_{11}, and P_{13} waves are determined from the data fit using eqs. (24-26). One overall phase remains undetermined, we set the S_{11} phase to zero. The amplitude and phase errors correspond to an increase of the full χ^2 by 1 when the plotted parameter (magnitude or phase) is changed

Table 1. Quality of the S and P waves energy independent fit: $\chi^2/N_{\rm data}$ and number of data points (in brackets). The overall $\chi^2/N_{\rm data}$ is 1.41

Energy bin	ANL75 $d\sigma/d\Omega$	ANL75 $Pd\sigma/d\Omega$	RAL78 $d\sigma/d\Omega$	RAL78 P
1630 - 1650	0.8 (20)	1.3 (10)	0.2 (5)	0.16 (5)
1650 - 1670	0.5 (20)	0.6(10)	0.9 (10)	0.5 (10)
1670 - 1690	0.7 (160)	0.9(80)	1.0 (10)	1.2 (10)
1690 - 1710	1.4 (80)	0.5(40)	10 (9)	2.4 (9)
1710 - 1730	-	-	0.8 (10)	2.8 (14)
1750 - 1770	-	-	1.8 (10)	4.3 (14)
1790 - 1810	-	-	2.0 (10)	4.7 (14)
1810 - 1830	-	-	2.2 (10)	5.1 (14)

and all other parameters are refitted. From the best fit we use eqs. (28 -30) for a numerical search for further solutions. Even in this simplest case there is no unambiguous solution. For each energy bin, we found two different physical solutions.

For every energy bin, one of the two solutions can be chosen, giving a multitude of different energy dependencies of the three amplitudes. In Fig. 2 the two solutions are sorted according their proximity (in terms of χ^2) to the energy dependent solution BnGa2011-02. The "best" solution agrees moderately well with BnGa2011-02 with $\chi^2/N = 262/40$.

The left column in Fig. 2 shows the energy independent solution (represented by "data" points with error bars) where the three magnitudes and the two phases are better compatible with the energy dependent solution (represented by the curves). The S_{11} and P_{11} amplitudes are reasonably consistent with the energy dependent fit even though the phase of the P_{11} wave shows some discrepancy. The P_{13} magnitude is overestimated over a wide energy range, this could be due to the neglect of higher waves.

The two solutions have similar S_{11} amplitudes even though the threshold behavior is different. Sizable differences are seen in the magnitudes of the P_{11} and P_{13} amplitudes. Solution 1 is close to the energy-dependent solution but the analysis suggest that the energy depend fit might underestimate the P_{13} amplitude.

Table 2. Quality of the S, P and D waves energy independent fit: $\chi^2/N_{\rm data}$ and number of data points (in brackets). The overall $\chi^2/N_{\rm data}$ is now 0.98

Energy bin	ANL75 $d\sigma/d\Omega$	ANL75 $Pd\sigma/d\Omega$	RAL78 $d\sigma/d\Omega$	RAL78 P
1630-1650	0.8 (20)	1.3(10)	0.15 (5)	0.06 (5)
1650-1670	0.6 (20)	0.6(10)	0.8 (10)	0.6 (10)
1670-1690	0.65 (160)	0.8(80)	0.75 (10)	1.0 (10)
1690-1710	1.2 (80)	0.5(40)	10 (9)	1.0 (9)
1710-1730	-	-	0.2 (10)	1.15 (14)
1750-1770	-	-	0.4 (10)	1.6 (14)
1790-1810	-	-	0.7 (10)	1.5 (14)
1810-1830	-	-	0.5 (10)	1.5 (14)

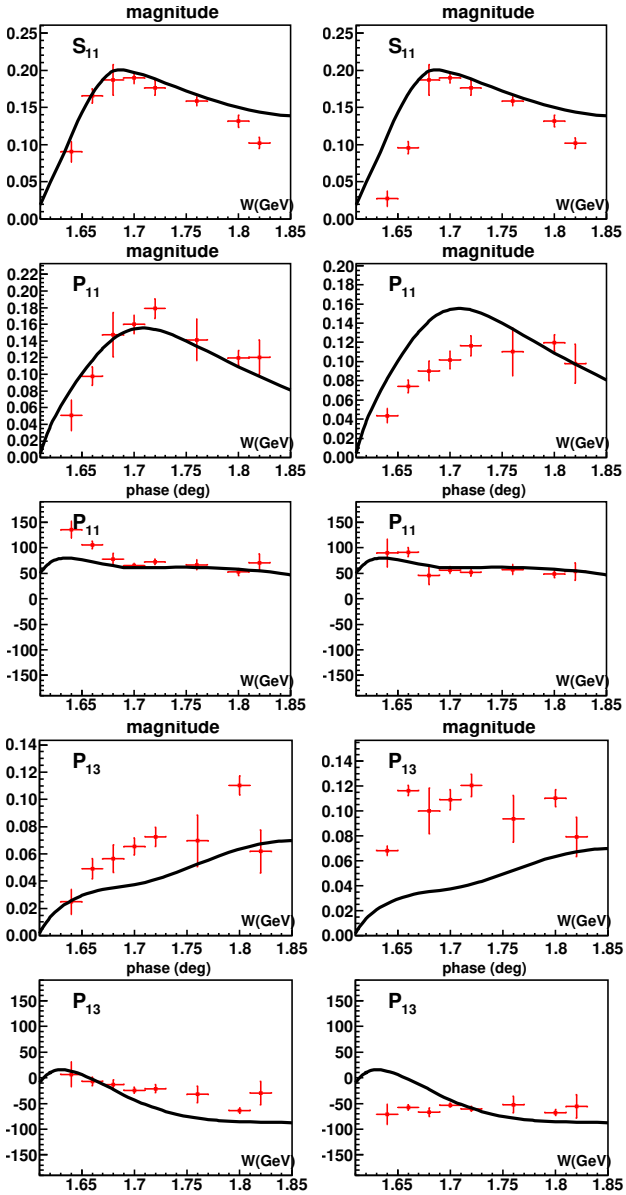

Fig. 2. Two solutions (left and right) for the decomposition of the $\pi N \to \Lambda K$ scattering amplitude with S and P waves. A large number of further solutions can be drawn by arbitrary choices of points from the left or right sub-figure. The solid line is the energy dependent solution BnGa2011-02.

In the 1690 to 1710 MeV mass slice, the differential cross section $d\sigma/d\Omega$ from ANL75 [8] and RAL78 [9] are not consistent. To study the importance of this effect, we left out the ANL75 data [8]. The reconstructed amplitudes changed a bit, the error bars increased but the conclusions remained unchanged.

3.2 Energy independent PWA near threshold with S, P and D waves

A better fit to the data can be achieved when D waves are admitted in addition to S and P waves. The fit is shown in Fig. 1 as solid line, the χ^2 of the fit is given in Table 2. The quality of the fit is now acceptable but the price one has to pay is

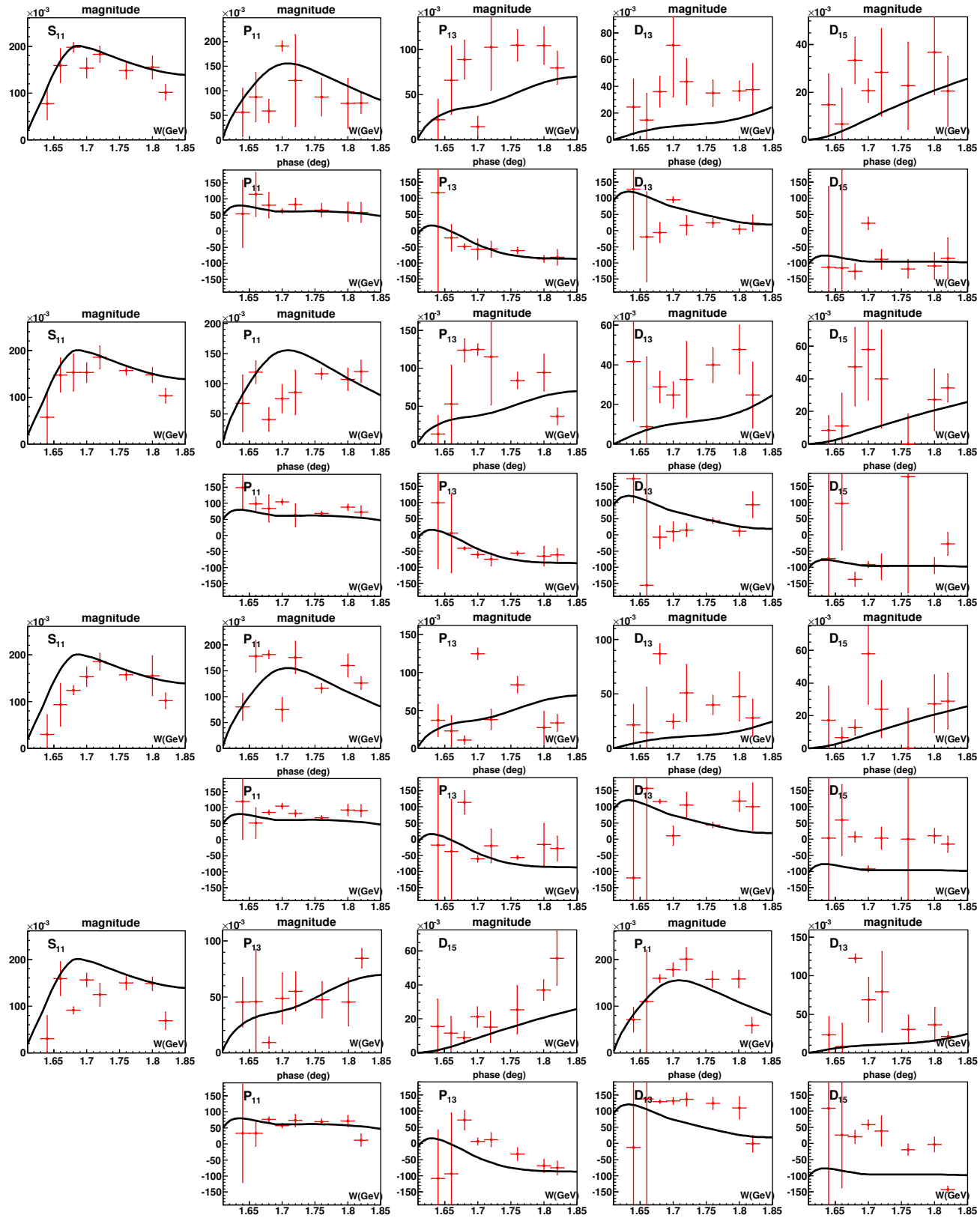

Fig. 3. Ambiguous solutions for the decomposition of the $\pi N \to \Lambda K$ scattering amplitudes with S, P and D waves. The solid line is the energy dependent solution BnGa2011-02. The first solution given in the first two lines is chosen as the closest to the energy-dependent fit. The solutions 2 to 6 given in the subsequent pairs of lines differ from the energy-dependent fit with increasing χ^2. The "best" solution agrees with the BnGa energy dependent fit with $\chi^2/N = 188/72$. There is a multitude of further solutions: one may taken seven (or six, $\cdots$) energy points from the first solution and the missing points from the second (or third, $\cdots$) solution to obtain additional solutions.

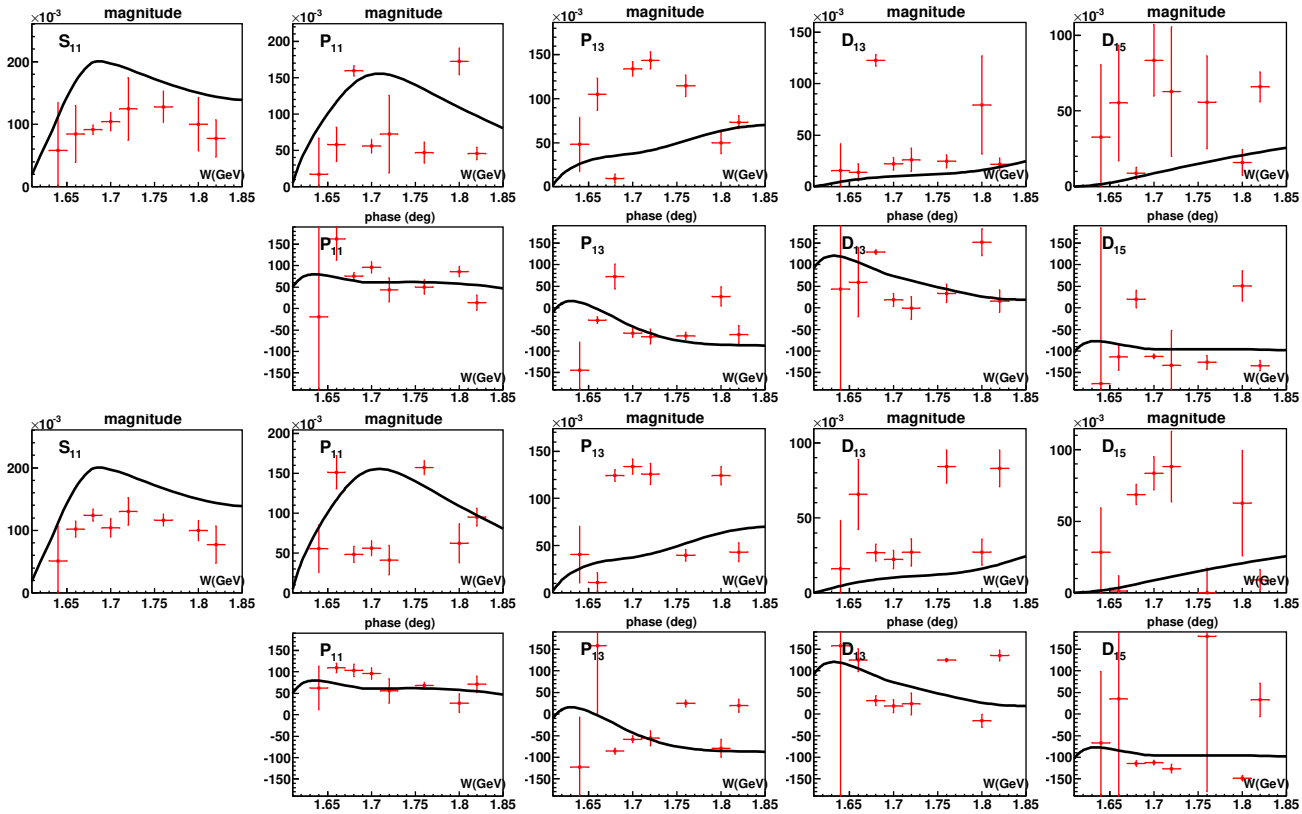

Fig. 3 continued.

the increase in the number of ambiguous solutions. Numerically, we now find, for each energy bin, six different solutions. Again, these are sorted according to their proximity to the energy dependent solution, starting from the upper row on Fig. 3. The total number of possible solutions is much larger than 6: At each energy, there are 6 independent solutions, and they can be combined in any order. Without the *a priori* knowledge of an energy independent solution, there seems to be little chance to choose the correct solution among the numerous ambiguous solutions which all reproduce the data with exactly the same χ^2.

The second price for the inclusion of D-waves are much larger error bars of the amplitudes. The two newly added amplitudes D_{13} and D_{15} are smaller by nearly one order of magnitude when compared to the leading S_{11} wave, and the energy dependent fit overestimates their contributions.

It may be surprising that not only the amplitudes, moduli and phases, are different in the six solutions but also their errors. This is due to the fact that the different solutions are often close to each other; depending on small details, the fit may identify a clear minimum or find an effective minimum of two or more close-by minima.

4 Energy independent PWA in the $1840 - 2270$ MeV region

In the region $1840 - 2270$ MeV region, a *complete* experiment has been performed; differential cross section $d\sigma/d\Omega$, Λ polarization P, and spin-rotation angle β were measured [9,10,11]. From these data we select 7 bins of $10 - 20$ MeV width which have all three experimental observables. The complete data set eliminates the ambiguities which we have near threshold. The only ambiguities we could have now are related to the quality of the data. Let us note at this point that β has be measured only in a limited range of angles ($\cos\theta \geq 0$). The very rapid changes or even the discontinuities of the β observable happens at points where $P^2 \approx 1$ and where both observables, R and A, are small. If they both change the sign, the phase of β varies by 180 degrees.

4.1 Solution with S,P and D waves

As the first step, we fit the data with S, P and D waves. The fit is shown in Fig. 4 as dotted curve, the quality of the fit in terms of χ^2's is given in Table 3. The fit to the differential cross sections is satisfactory, partly even excellent. More problems originate from the polarization variables: through interference, they are more sensitive to the presence of small waves. In particular the β parameter is badly described.

The resulting amplitudes are shown in Fig. 5. Magnitudes and phases of the reconstructed amplitudes resemble only vaguely the curves representing the energy dependent fit. We anticipate the need of higher partial waves with $L > 2$.

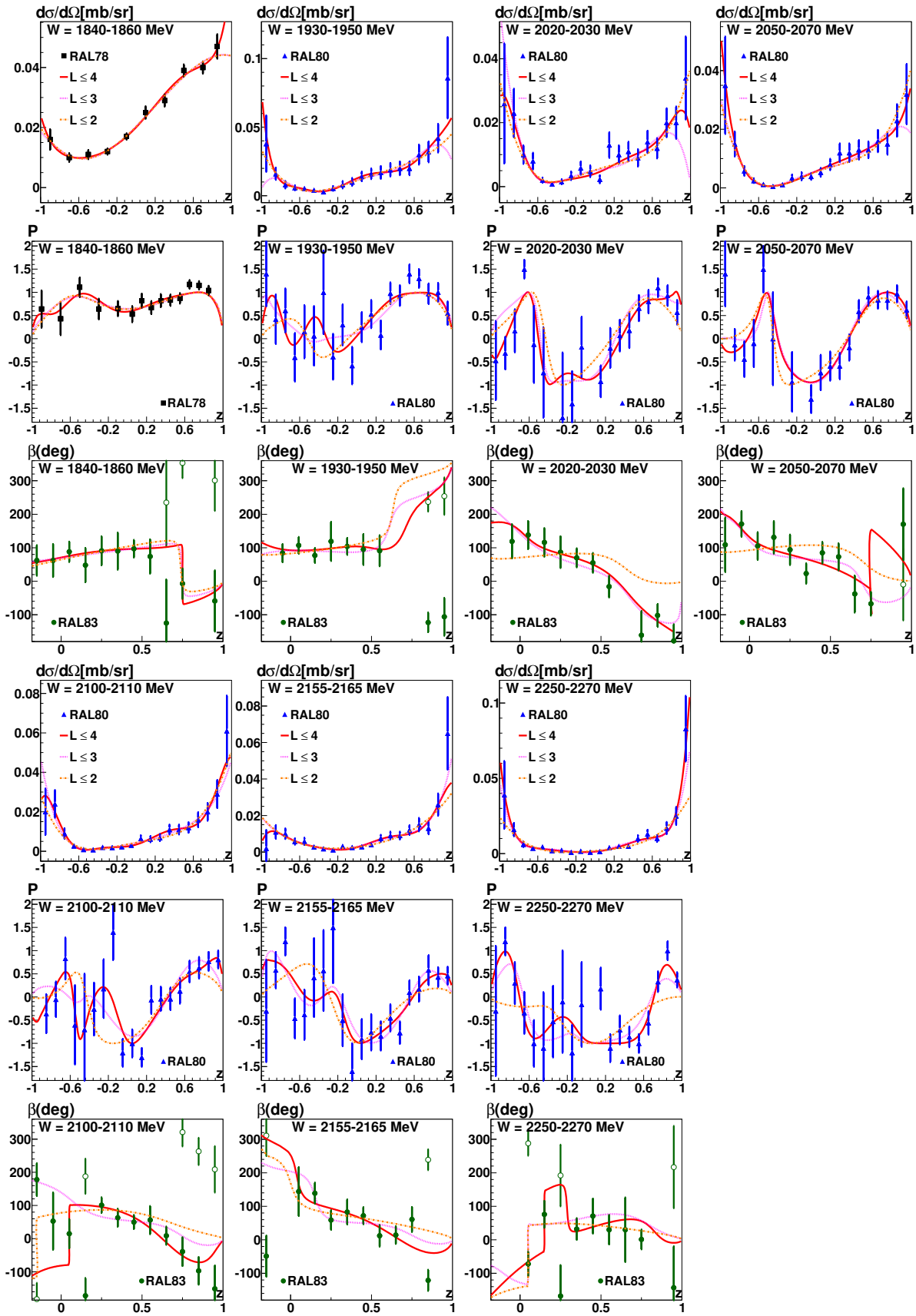

Fig. 4. Energy independent fit (red lines) for $\pi^- p \to K^0 \Lambda$ reaction in the region $1840-2270$ MeV. The experimental data are from RAL78 [9], RAL80 [10], and RAL83 [11]. Note that β is 360-degree cyclic which leads to additional data points shown by empty circles. The BnGa2010-02 fit to the data is shown in figs. 1 - 4 of [15].

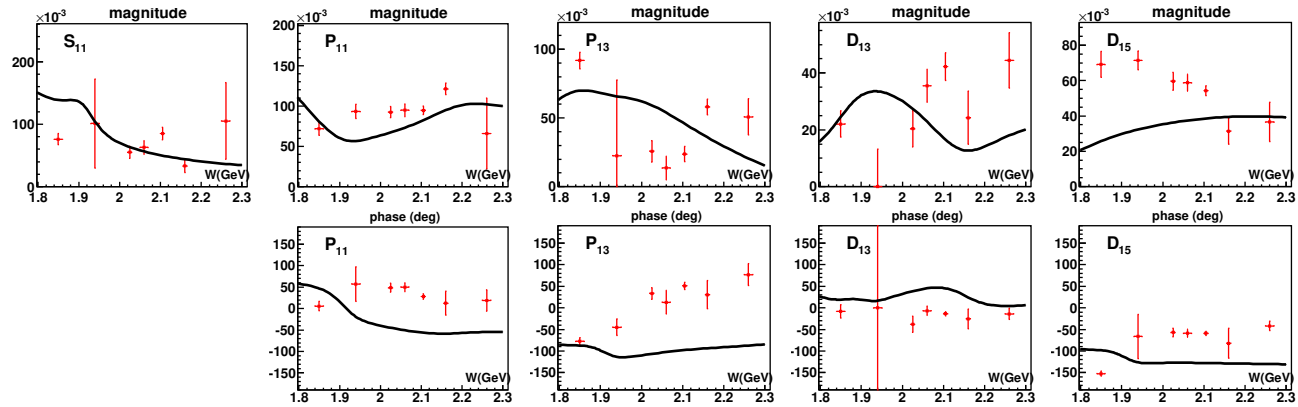

Fig. 5. Decomposition of the $\pi N \to \Lambda K$ scattering amplitudes with S, P, and D waves. The solid line is the energy dependent solution BnGa2011-02. There is no good agreement between the energy dependent and independent solutions, $\chi^2/N = 1982/63$.

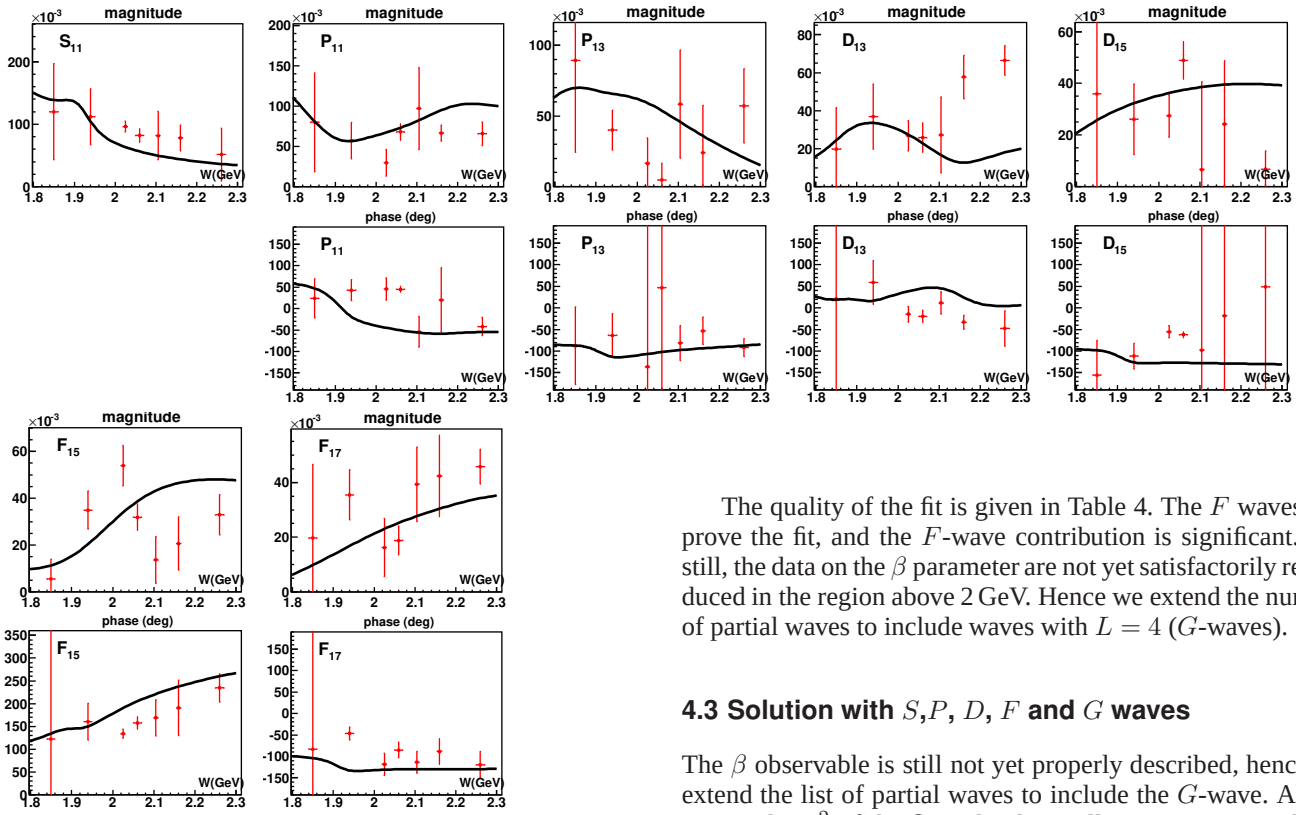

Fig. 6. Decomposition of the $\pi N \to \Lambda K$ scattering amplitudes with S, P, D, and F waves. The solid line is the energy dependent solution BnGa2011-02. There is still no good agreement between the energy dependent and independent solutions, $\chi^2/N = 868/91$.

4.2 Solution with S,P, D and F waves

As the next step, we include additionally F waves in the energy independent PWA. The dashed curve in Fig. 4 represents this fit. The scattering amplitudes in this case (with S,P, D, and F waves included) are shown in Fig. 6. The amplitude errors are again obtained from solutions which differ from the best solution by $\delta\chi^2 < 1$.

The quality of the fit is given in Table 4. The F waves improve the fit, and the F-wave contribution is significant. But still, the data on the β parameter are not yet satisfactorily reproduced in the region above 2 GeV. Hence we extend the number of partial waves to include waves with $L = 4$ (G-waves).

4.3 Solution with S,P, D, F and G waves

The β observable is still not yet properly described, hence we extend the list of partial waves to include the G-wave. Above 2 GeV, the χ^2 of the fit to the data still improves, see Table 5 and the solid line in Fig. 4.

The G waves are small, but their inclusion clearly changes the energy independent solution in other waves. Even in the S_{11} wave energy dependent and independent solutions are now no longer consistent. Of course, the large errors of the scattering amplitudes are the result of the poor quality of the experimental data. While the data seem to require even $L = 4$ waves, their inclusion leads to large uncertainties in scattering amplitudes. These are shown in Fig. 7.

4.4 Error bands

A major source of uncertainty is the absence of the spin rotation data in the region $z < -0.2$. To illustrate this uncertainty

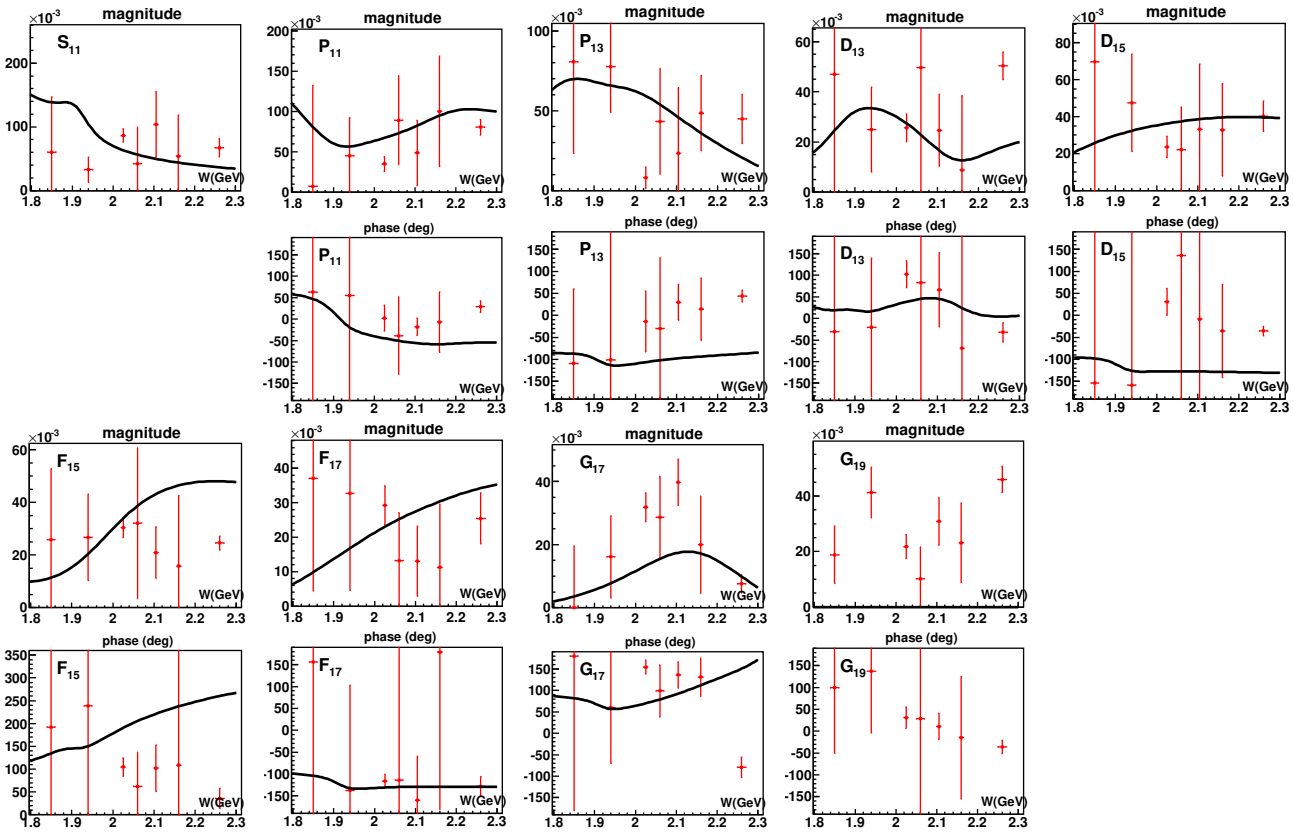

Fig. 7. Decomposition of the $\pi N \to \Lambda K$ scattering amplitudes with S, P, D, F and G waves. The solid line is the energy dependent solution BnGa2011-02. The agreement between the energy dependent and independent solutions has become worse due to an increase of random fluctuations; $\chi^2/N = 1966/105$.

the error bands for A and R observables were defined which include the solutions with $\delta\chi^2 < 1$ from the best one. They are shown in Fig. 8. We use the fits with $L \leq 4$ since they show best the angular ranges where more precise data are urgently needed.

4.5 Fits with fixed high or low partial waves.

Having all partial waves free in the fits leads to very large errors and the results are of no use any longer. Apparently, the statistical accuracy of the data is not sufficient to extract all partial waves simultaneously. We therefore fixed the D, F, and G waves to the energy dependent solution, and then determined the energy independent amplitudes from a fit to the data. The result is shown in Fig. 9. The results now look reasonable, but suggest that the transition matrix element for the P_{13} wave in $\pi^- p \to \Lambda K^0$ could be larger than the value found from the energy dependent fit. This matrix element is, however, well fixed from the reactions $\gamma p \to p\pi^0$, $\gamma p \to n\pi^+$, and $\gamma p \to \Lambda K^+$ which have much higher statistics. Hence we refrain from an overall refit of the data imposing the new energy independent solution shown in Fig. 6.

Alternatively, we may ask if the high partial waves can be determined from the data, once the low partial waves are fixed. Thus we constrained the low partial waves (S and P-waves) to coincide with the energy-dependent solution BnGa2011-02 while the high waves were left free in the fit to reproduce the data on $\pi^- p \to \Lambda K^0$. The resulting amplitudes are shown in Fig. 10. The results still have large error bars but are mostly not inconsistent with the energy-dependent solution.

5 Summary and Conclusions

We have studied the ambiguity problem which arises when incomplete data are used to derive complex scattering amplitudes. We use existing data on pion-induced production of Λ hyperons. In the low energy region, data for this reaction exist on the differential cross section and Λ polarization.

Assuming that only S and P waves contribute, the data can be described with sufficient accuracy up to 1700 MeV in invariant mass. The reconstructed magnitudes of the P_{11} and S_{11} waves, defined to be close to the energy dependent solution, are consistent with the results from the energy dependent analysis, see Fig. 9; the P_{11} - S_{11} phase difference might indicate problems in the ΛK threshold region (see Fig. 2, left column). The P_{13} wave seems to be overestimated in the energy independent fit. The P_{13} phase motion (relative to the S_{11} phase) does, however, not support any additional feature atop of the known resonances. If D waves are admitted, the number of numerically different solution increases to six. The "best" solution (the two

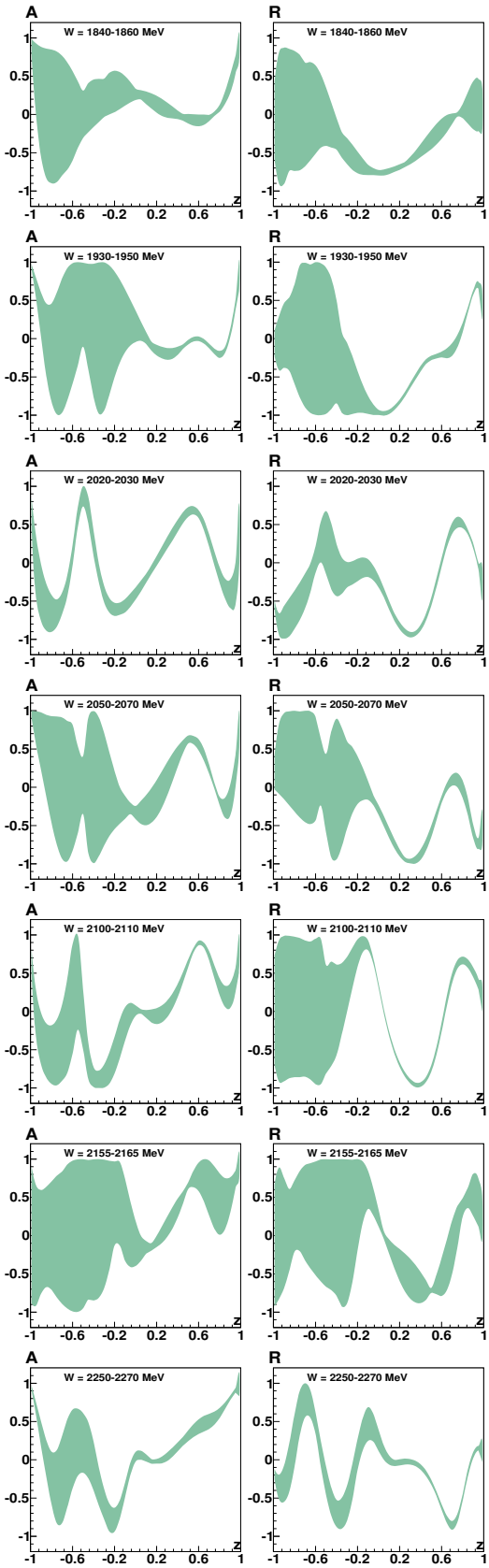

Fig. 8. Error bands for A and R observables for the best energy independent fit with $L \leq 4$

top rows in Fig. 3) is reasonably consistent with the predicted curves even though most waves show large error bars and an excess in magnitude of the reconstructed amplitudes.

Above 1800 MeV, up to 2270 MeV in total energy, the spin rotation angle β has been determined and nearly complete information exists even though not with complete solid angle coverage. The scattering amplitudes can now be reconstructed unambiguously. If only S, P, and D are admitted, large discrepancies show up between energy independent and energy dependent amplitudes (see Fig. 5). Apparently, the angular distributions require at least F waves, and even G waves improve the quality of the fit substantially. However, the errors of magnitude and phase of the reconstructed amplitudes become increasingly larger.

Approximate consistency between the energy-dependent and independent solution can be obtained by providing some *guidance* to the fit by fixing the low-energy partial waves or the high-energy partial waves, and then determining the other partial waves from a fit to the data. This *guidance* leads to reasonably looking results in particular for the low waves (see Fig. but clearly,the final result on the energy-independent solution is strongly biased by the energy-dependent solution. In the present case, in the study of $\pi^- p \to \Lambda K^0$, the energy-independent approach does not yield information which goes beyond the information already provided by the energy-dependent solution.

The final aim of this development is the reconstruction of amplitudes from photoproduction data. This is an even more demanding task but the data will have (and need to have) much smaller statistical and systematic errors. If this can be achieved,

Table 3. Quality of the energy independent fit in the region $1840 - 2270$ MeV using S, P and D waves: $\chi^2/N_{\rm data}$ and number of data points (in brackets). The overall $\chi^2/N_{\rm data}$ is 1.52.

Energy bin	$d\sigma/d\Omega$	P	β
1840-1860	0.45 (10)	0.92 (14)	0.50 (11)
1930-1950	0.38 (20)	1.19 (20)	1.53 (9)
2020-2030	1.08 (20)	1.71 (19)	4.06 (10)
2050-2070	0.42 (20)	1.00 (18)	3.12 (11)
2100-2110	0.64 (20)	2.60 (20)	4.02 (12)
2155-2165	0.75 (20)	1.65 (20)	3.24 (10)
2250-2270	1.28 (20)	4.46 (19)	0.97 (9)

Table 4. Quality of the S, P, D and F waves energy independent fit in the region $1840 - 2270$ MeV: $\chi^2/N_{\rm data}$ and number of data points (in brackets). The overall $\chi^2/N_{\rm data}$ is now 0.97.

Energy bin	$d\sigma/d\Omega$	P	β
1840-1860	0.46 (10)	0.91 (14)	0.41 (11)
1930-1950	0.49 (20)	0.96 (20)	0.46 (9)
2020-2030	1.16 (20)	1.52 (19)	0.58 (10)
2050-2070	0.43 (20)	0.76 (18)	1.99 (11)
2100-2110	0.45 (20)	1.97 (20)	3.55 (12)
2155-2165	0.53 (20)	0.93 (20)	4.07 (10)
2250-2270	0.73 (20)	1.78 (19)	1.32 (9)

the data will return amplitudes from which the spectrum of nucleon and Δ resonances can be deduced unambiguously.

Acknowledgements

We acknowledge financial support from the Deutsche Forschungsgemeinschaft within the Sonderforschungsbereich SFB/TR16 (DFG). This work is also supported by Russian Foundation for Basic Research 13-02-00425 .

References

1. H. Arenhovel, W. Leidemann and E. L. Tomusiak, Nucl. Phys. A **641**, 517 (1998).
2. G. Höhler, F. Kaiser, R. Koch and E. Pietarinen, "Handbook Of Pion Nucleon Scattering," Published by Fachinform. Zentr. Karlsruhe 1979, 440 P. (Physics Data, No.12-1 (1979)).
3. G. Höhler, πN Newslett. **9**, 108 (1993).
4. R. E. Cutkosky *et al.*, "Pion - Nucleon Partial Wave Analysis," 4th Int. Conf. on Baryon Resonances, Toronto, Canada, Jul 14-16, 1980. Published in Baryon 1980:19 (QCD161:C45:1980)
5. R. A. Arndt, W. J. Briscoe, I. I. Strakovsky and R. L. Workman, Phys. Rev. C **74**, 045205 (2006).
6. M. Shrestha and D. M. M. Manley, Phys. Rev. C **86**, 045204 (2012).
7. M. Shrestha and D. M. Manley, Phys. Rev. C **86** (2012) 055203.
8. T. M. Knasel *et al.*, Phys. Rev. D **11**, 1 (1975).
9. R. D. Baker *et al.*, Nucl. Phys. B **141**, 29 (1978).
10. D. H. Saxon *et al.*, Nucl. Phys. B **162**, 522 (1980).
11. K. W. Bell *et al.*, Nucl. Phys. B **222**, 389 (1983).
12. A. Gersten, Nucl. Phys. B **12**, 537 (1969).
13. E. Barrelet, Nuovo Cim. A **8** (1972) 331.
14. R. D. Baker, "Barrelet Zeros in Partial Wave Analysis," RL-76-013.

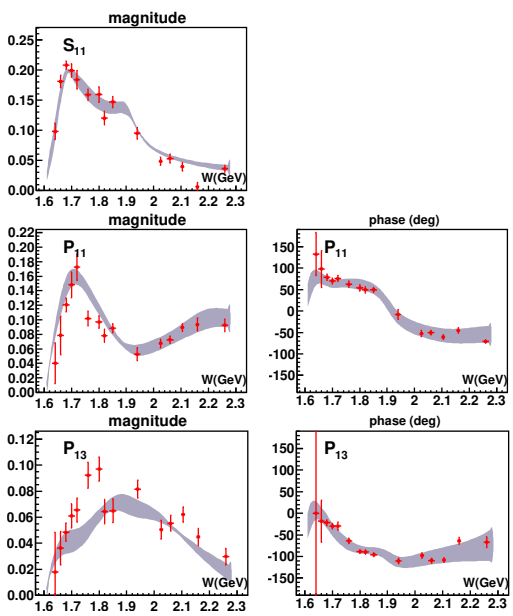

Fig. 9. Fit with free S and P-waves and D, F, and G-waves fixed to the energy-dependent solution BnGa2011-02.

Table 5. Quality of the S, P, D, F and G waves energy independent fit in the region $1840 - 2270$ MeV: $\chi^2/N_{\rm data}$ and number of data points (in brackets). The overall $\chi^2/N_{\rm data}$ is now 0.67.

Energy bin	$d\sigma/d\Omega$	P	β
1840-1860	0.31 (10)	0.87 (14)	0.20 (11)
1930-1950	0.14 (20)	0.92 (20)	0.23 (9)
2020-2030	1.03 (20)	1.06 (19)	0.40 (10)
2050-2070	0.28 (20)	0.78 (18)	0.74 (11)
2100-2110	0.29 (20)	1.22 (20)	1.09 (12)
2155-2165	0.61 (20)	0.83 (20)	1.54 (10)
2250-2270	0.49 (20)	0.77 (19)	0.63 (9)

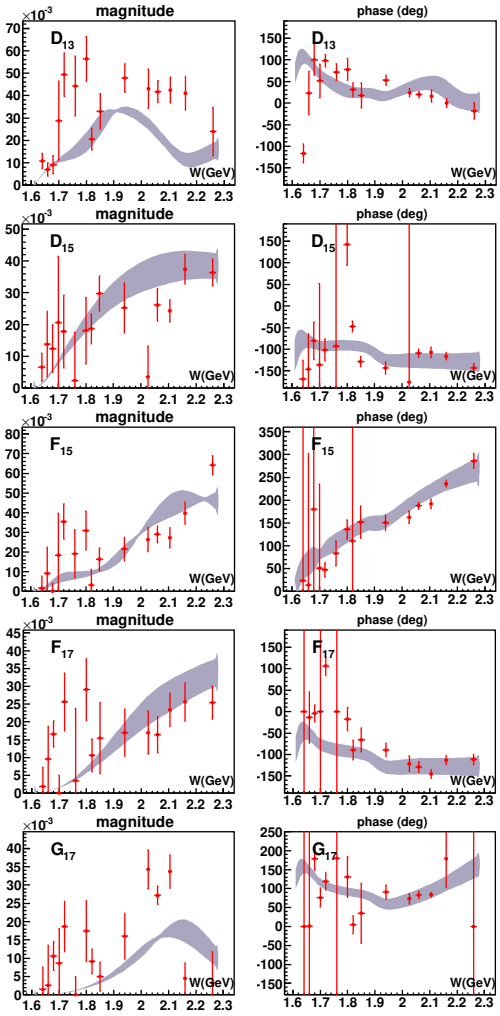

Fig. 10. Fit with free D, F, and G-waves and S and P-waves fixed to the energy-dependent solution BnGa2011-02.

15. A. V. Anisovich, E. Klempt, V. A. Nikonov, A. V. Sarantsev and U. Thoma, Eur. Phys. J. A **47**, 27 (2011).
16. A. V. Anisovich, R. Beck, E. Klempt, V. A. Nikonov, A. V. Sarantsev and U. Thoma, Eur. Phys. J. A **48**, 15 (2012).